ARTICLES
PUBLISHED ONLINE: 20 NOVEMBER 2011 | DOI: 10.1038/NGEO1324
nature geoscience

Large inert carbon pool in the terrestrial biosphere during the Last Glacial Maximum

P. Ciais[1]*, A. Tagliabue[1†], M. Cuntz[2,3], L. Bopp[1], M. Scholze[4], G. Hoffmann[1], A. Lourantou[1], S. P. Harrison[5,6], I. C. Prentice[5,7], D. I. Kelley[5,6], C. Koven[1,9] and S. L. Piao[8]

During each of the late Pleistocene glacial–interglacial transitions, atmospheric carbon dioxide concentrations rose by almost 100 ppm. The sources of this carbon are unclear, and efforts to identify them are hampered by uncertainties in the magnitude of carbon reservoirs and fluxes under glacial conditions. Here we use oxygen isotope measurements from air trapped in ice cores and ocean carbon-cycle modelling to estimate terrestrial and oceanic gross primary productivity during the Last Glacial Maximum. We find that the rate of gross terrestrial primary production during the Last Glacial Maximum was about 40 ± 10 Pg C yr^{-1}, half that of the pre-industrial Holocene. Despite the low levels of photosynthesis, we estimate that the late glacial terrestrial biosphere contained only 330 Pg less carbon than pre-industrial levels. We infer that the area covered by carbon-rich but unproductive biomes such as tundra and cold steppes was significantly larger during the Last Glacial Maximum, consistent with palaeoecological data. Our data also indicate the presence of an inert carbon pool of 2,300 Pg C, about 700 Pg larger than the inert carbon locked in permafrost today. We suggest that the disappearance of this carbon pool at the end of the Last Glacial Maximum may have contributed to the deglacial rise in atmospheric carbon dioxide concentrations.

The increase of nearly 100 ppm in atmospheric CO_2 observed during repeated glacial–interglacial transitions still awaits a comprehensive explanation. This problem has major implications for assessments of long-term future changes in the carbon cycle; it implies the existence of a 'phase transition' in the coupled climate–carbon system that was repeatedly crossed, but which cannot be simulated by present models. Tackling this enigma requires a better understanding of past reorganizations in the coupled carbon–climate system and redistributions among the carbon reservoirs during glacial–interglacial transitions.

Although the distribution of carbon stocks and fluxes during the pre-industrial period (PRE) is relatively well known[1], the state of the carbon cycle during the Last Glacial Maximum (LGM) is more controversial. Early estimates[2,3] of the difference in terrestrial carbon stocks (LGM − PRE) ranged from −1,200 Pg C to +50 Pg C. More recent and presumably more realistic calculations[4–9] give a smaller range, of 0 Pg C to 700 Pg C, but large uncertainties remain. Increased terrestrial carbon stocks during interglacial periods require the ocean to have outgassed more carbon than would be inferred from the atmospheric CO_2 signal alone, owing to an increasing land sink. Insufficient constraints on the carbon cycle at the LGM preclude a clear understanding of the contribution of the ocean and terrestrial reservoirs to the atmospheric CO_2 increase.

Reconstructing the LGM carbon cycle from necessarily sparse observations is challenging. On land, pollen and macrofossil data provide information about the extent and composition of different biomes[10–12], but such data alone cannot reliably be used to infer terrestrial carbon fluxes or pool sizes. Terrestrial-biosphere model calculations are impacted by uncertainties in climate forcing[11] and differences in the modelled response of the LGM vegetation distribution and carbon cycling to a colder, drier, low-CO_2 environment[10,13]. The present generation of biosphere models are likely to be biased towards low total terrestrial carbon stocks, for instance because they do not account for the carbon stored in deep permafrost soils, in northern peatlands[14], and maybe in tropical wetlands[15].

Marine-sediment records provide information about the broad features of the changes in ocean circulation and properties, but observations directly relevant to the global carbon cycle are scarce and have not been fully exploited[16]. Ocean carbon model simulations[17–19] indicate that ocean productivity GPP_{OCEAN} and carbon stock M_{OCEAN} estimates during the LGM are sensitive to assumptions related to thermohaline ventilation rates, deposition of terrigeneous iron from dust and the effects of iron deposition on the composition and primary production of phytoplankton communities. Most studies of LGM ocean carbon cycle quantitatively have used either box models[18] or intermediate complexity models[19] that do not allow the detailed spatial comparison with palaeo-data for evaluation of their conclusions. A recent analysis using three-dimensional model ensemble simulations of ocean circulation and biology concluded that the modelled ocean carbon stock is particularly sensitive to changes in palaeoproductivity[17]. Evidently, the LGM carbon cycle in the ocean also needs to be constrained by independent, global observations.

[1]Laboratoire des Sciences du Climat et de l'Environnement, CEA-CNRS-UVSQ, CE Orme des Merisiers, 91191 Gif sur Yvette Cedex, France, [2]UFZ—Helmholtz Centre for Environmental Research, Permoserstr. 15, 04318 Leipzig, Germany, [3]Max-Planck Institute for Biogeochemistry, Hans-Knöll-Str. 10, 07745 Jena, Germany, [4]Department of Earth Sciences, University of Bristol, Wills Memorial Building, Queens Road, Bristol BS8 1RJ, UK, [5]Department of Biological Sciences, Macquarie University, North Ryde, New South Wales 2109, Australia, [6]School of Geographical Sciences, University of Bristol, Bristol BS8 1SS, UK, [7]Grantham Institute for Climate Change, and Division of Biology, Imperial College, Silwood Park Campus, Ascot SL5 7PY, UK, [8]Department of Ecology, College of Urban and Environmental Science, Peking University, Beijing 100871, China, [9]Lawrence Berkeley National Laboratory, 1 Cyclotron Road, MS 50-4037, Berkeley, California 94720, USA. †Present address: Southern Ocean Carbon and Climate Observatory, CSIR, PO Box 320, Stellenbosch, 7599, South Africa. *e-mail: philippe.ciais@lsce.ipsl.fr.

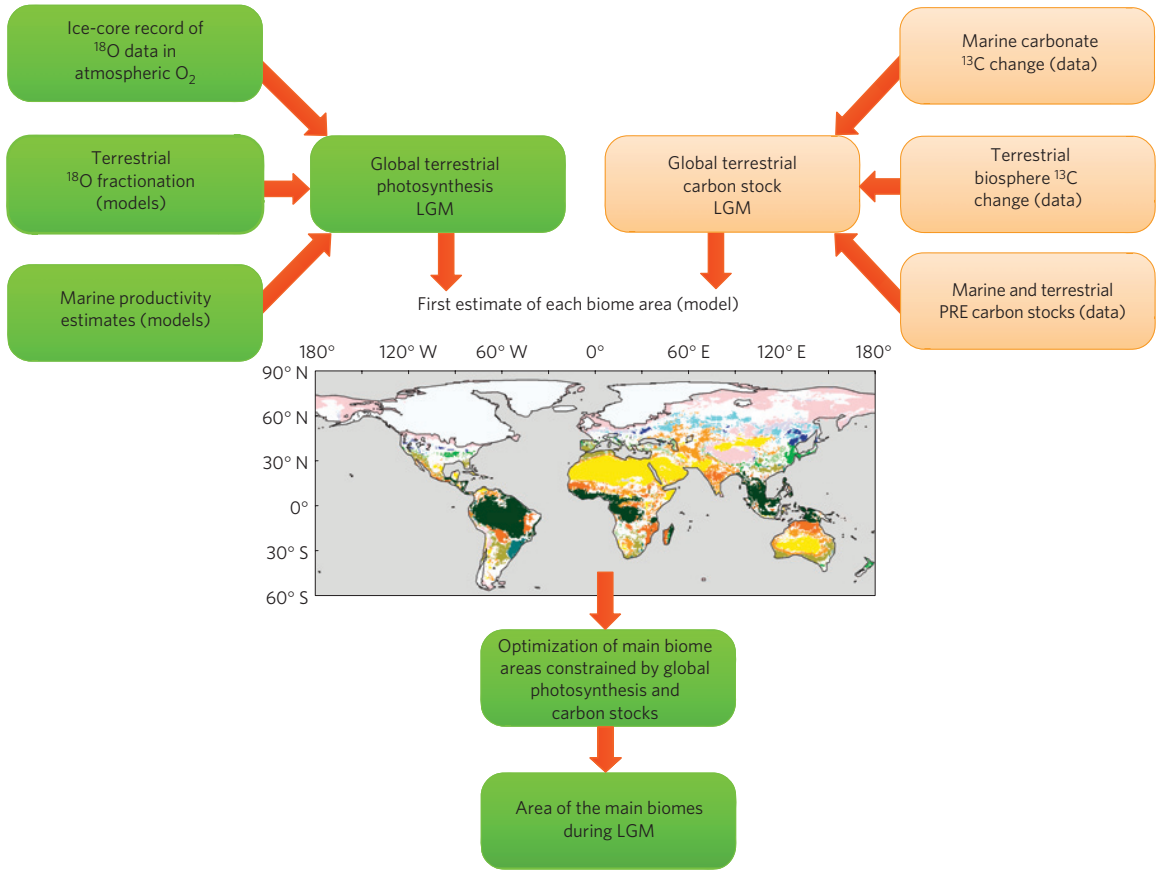

Figure 1 | Overview of observations and model results used to constrain during the LGM, global estimates of terrestrial photosynthesis, and of marine and terrestrial carbon stocks. These global estimates are combined with results from a land-biosphere model to optimize areas of five 'mega-biomes' during the LGM. More details on this calculation are given in the text, Methods and Supplementary Information.

The goal of this paper is to reconstruct marine and terrestrial productivity and carbon stocks at the LGM, by combining isotope data that are relevant to global quantities, and global models. We use ^{18}O in molecular oxygen (O_2) measurements from ice-core records to reconstruct terrestrial gross primary production (GPP_{TER}) and ^{13}C in ocean sediment cores, and in atmospheric CO_2 (ice cores) to quantify carbon stocks in land ecosystems versus the ocean. The steps in our reconstruction are presented in Fig. 1.

Terrestrial photosynthesis from oxygen isotopes

Atmospheric O_2 is characterized by a large isotopic enrichment in ^{18}O when compared with sea water. This enrichment is known as the Dole effect[20,21] ($DE = \delta^{18}O_{O2\text{-atmosphere}} - \delta^{18}O_{seawater}$). It arises because both land and ocean photosynthetic O_2 emissions fractionate ^{18}O relative to ^{16}O, with the heavier molecules being left behind in the atmosphere[22]. Oxygen emitted by land photosynthesis is further enriched in ^{18}O by isotopically heavy water derived from the soil, whose signature is transferred to leaves through the transpiration stream[23]. The amount and patterns of leaf water enrichment depend on rainwater isotopic composition and atmospheric dryness[24,25].

The Dole effect can be tracked through time by measuring the ^{18}O content of O_2 preserved in air bubbles trapped in ice cores. It is linearly related to the ocean and the land GPP, GPP_{OCEAN} and GPP_{TER}, respectively[22] (Methods). We estimate a range of GPP_{OCEAN} of 110 ± 30 Pg C yr^{-1} using different ocean carbon-cycle models[17–19,26,27] for the LGM (Methods and Supplementary Table S1). The two parameters that allow us to infer GPP_{TER} from ice-core ^{18}O measurements given GPP_{OCEAN} (Fig. 2) are the isotopic enrichments implied by land fluxes, DE_{TER}, and by ocean fluxes, DE_{OCEAN}. We calculated these two parameters with a global model of carbon and oxygen biogeochemical cycles[28] (Methods).

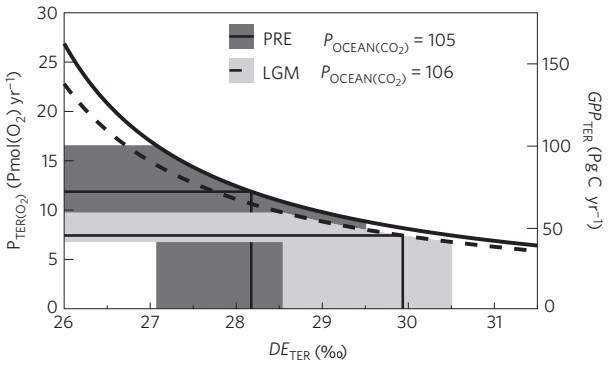

Figure 2 | Relationship defining terrestrial photosynthesis (GPP_{TER}) as a function of the ^{18}O isotopic enrichment of land oxygen fluxes, or land Dole effect, DE_{TER}. Simulations of DE_{TER} for the PRE (dark grey) and LGM (light grey), together with measurements of ^{18}O in atmospheric oxygen from ice cores, allow GPP_{TER} during the LGM to be constrained. $P_{TER(O2)}$ is the global flux of oxygen (left-hand axis) emitted by terrestrial photosynthesis, about two times GPP_{TER}. The lines depend on ocean productivity for the PRE (solid) and LGM (dashed). Shaded grey uncertainties are calculated with Monte Carlo analysis of ocean and land parameters (see Supplementary Information).

Global terrestrial GPP today[29] is in the region of 110–130 Pg C yr^{-1}. We infer that GPP_{TER} was 80 ± 30 Pg C yr^{-1} during the PRE; that is, lower than today, possibly because of the

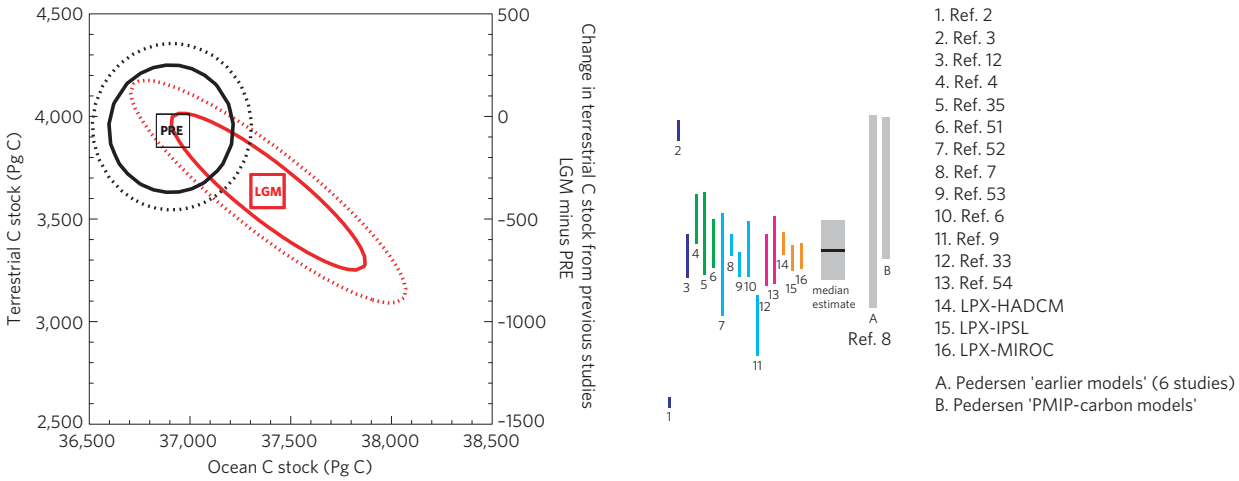

Figure 3 | Ocean and land carbon stocks inferred from carbon isotopes for the PRE and LGM. Uncertainties shown by ellipses are obtained by considering the error on each parameter entering the carbon isotope mass balance (see Supplementary Information). Solid lines are 1-σ uncertainty, and dotted lines are 2-σ uncertainty. Vertical colour bars on the right-hand side denote literature estimates of changes in global terrestrial carbon stock between the PRE and LGM. Blue (1–3), early work based on cartographic reconstructions (1) or modelling (2–3). Green (4–6), based on reconstruction of oceanic ^{13}C change, as in this study, but with older observations. Cyan (7–11), based on terrestrial-biosphere models and first-generation LGM climate models simulations from the PMIP-1 project. Magenta (12–13), based on ocean modelling. Orange (14–16), based on the LPX land-biosphere model forced by second-generation LGM climate model simulations from three models of the PMIP-2 program (those that had archived the necessary variables used to run LPX; see Supplementary Information). The grey bar is the median of estimates 1–16 plus or minus one median absolute deviation, excluding proven unrealistic estimates 1 and 2. The grey bars labelled A and B are the range of various published global terrestrial carbon stock values during the LGM from the review in ref. 8.

effect of anthropogenically increased CO_2 concentration on photosynthesis[10]. This pre-industrial GPP_{TER} estimate is lower than, but within the uncertainty range of, estimates from process-based models[30]. For the LGM, we found that $GPP_{TER} = 40 \pm 10$ Pg C yr^{-1}, that is, about half of the value for the PRE. GPP_{TER} was almost four times lower than GPP_{OCEAN} (110 ± 30 Pg C yr^{-1}) during the LGM. Accordingly, the ratio of total marine and terrestrial GPP between the LGM and PRE of 0.81 agrees with isotopic constraints from the triple isotope (^{18}O, ^{17}O, ^{16}O) composition of O_2 in ice cores (0.76–0.83; ref. 31), which provides an independent corroboration of our calculation. The smaller uncertainty obtained for GPP_{TER} during the LGM than for the PRE arises because a large uncertainty in modelled DE_{TER} scales into a smaller uncertainty in GPP_{TER} during the LGM owing to the curvature of the relationship shown in Fig. 2. From this, we infer a rough estimate of LGM terrestrial net primary production of 20 ± 10 Pg C yr^{-1} assuming a constant carbon-use efficiency of 50%. This estimate is lower than previously published estimates of net primary production from land-biosphere models during the LGM (28–40 Pg C yr^{-1}; refs 5,7).

LGM distribution of carbon stocks from carbon isotopes

Between the LGM and the pre-industrial Holocene, a redistribution of carbon stocks occurred between the atmospheric, land and ocean reservoirs. CO_2 uptake due to weathering of silicate rocks, and CO_2 emission from fluid–rock interactions and mantle outgassing, are small enough to be neglected on timescales of thousands (as opposed to millions) of years.

The clearest quantitative evidence for a glacial–interglacial redistribution of carbon among different carbon reservoirs is the deglacial rise in atmospheric CO_2 content as recorded by ice cores. However, this is not necessarily the largest signal, given that the land and ocean always store many times more carbon than the atmosphere. Evidence from previous studies indicates that the land biosphere contained between 300 and 700 Pg C less carbon during the LGM than during the pre-industrial Holocene[5,32,33] (Fig. 3). Outgassing of CO_2 from the ocean during the glacial–interglacial transition must then be large enough to supply a growing land biosphere, while also contributing to the observed increase in the atmospheric reservoir.

Using new palaeoproxy and modern data in the method developed in ref. 4 and on the basis of the hypothesis of invariance of global stocks of both ^{12}C and ^{13}C isotopes between the LGM and PRE, we infer that the LGM terrestrial carbon stock M_{TER} was $3{,}640 \pm 400$ Pg C; that is, only 330 Pg C less than during the pre-industrial Holocene (Table 1). Given the known change in atmospheric CO_2 content, it follows that the ocean carbon stock M_{OCEAN} was larger than today by 520 Pg C. We neglect in this calculation changes in ^{12}C and ^{13}C induced by significant changes of ocean carbonate formation, which would imply a change in the carbonate dissolution depth that is not observed, as well as changes in weathering that have been recently estimated to have a negligible contribution to the deglacial CO_2 rise.

The specific parameters needed in the mass-balance approach of ref. 4 for calculating M_{TER} and M_{OCEAN} are: PRE stocks in the land, and ocean reservoirs, the latter being estimated from ocean surveys, corrected for recent gains of anthropogenic carbon; PRE and LGM stocks in the atmosphere, obtained from ice-core records; changes in the ^{13}C isotopic composition of atmospheric CO_2 ($\Delta\delta_{ATM}$), obtained from ice-core recent measurements[34]; changes in the ^{13}C isotopic composition of oceanic dissolved inorganic carbon ($\Delta\delta_{OCEAN}$) estimated to be 0.34 ± 0.13‰ from a database of carbonates in 133 ocean cores (an alternative, but numerically similar, estimate is 0.31 ± 0.20‰, obtained from an ensemble of LGM ocean circulation simulations with a three-dimensional ocean model[17]); and changes in the isotopic composition of the terrestrial biosphere ($\Delta\delta_{TER}$) inferred to be 1 ± 1‰ from vegetation reconstructions[35,36] and from the results of a terrestrial-biosphere model of ^{13}C forced by simulated LGM climate anomalies from three climate models. More details on the parameters are given in the Supplementary Information.

Uncertainty in each parameter is propagated into the calculation of M_{TER} and M_{OCEAN} (equation (2) in Methods) and shown by the ellipses in Fig. 3. One key parameter of the mass-balance approach of ref. 4 that we re-estimate in this study is the PRE land carbon

Table 1 | Terrestrial and ocean carbon stocks, and global photosynthesis estimates for the LGM and PRE.

Time period	Carbon stocks (Pg C)						Photosynthesis (Pg C yr^{-1})	
	Land				Ocean	Atmosphere	Land	Ocean
	Sum of:	Land active	+	Land inert				
PRE	3,970 ± 325	2,370 ± 125	+	1,600 ± 300	36,830 ± 170	593 ± 2	80 ± 30	110 ± 30
LGM	3,640 ± 400	1,340 ± 500	+	2,300 ± 300	37,350 ± 400	399 ± 2	40 ± 10	110 ± 30
LGM minus PRE	−330	−1,030	+	700	520	−194	−40	0

Uncertainties are 1-σ estimates, and all numbers are rounded to 10. Note that the inferred terrestrial and ocean carbon stock estimates are anti-correlated; that is, a higher stock estimate for one reservoir immediately translates into a lower estimate for the other, as shown by the tilted ellipse in Fig. 3. For the PRE, the inert carbon pool corresponds to soil carbon in permafrost compiled by ref. 38. The active pool corresponds to all of the rest of the terrestrial biomass and soil carbon. For the PRE, the error on the global terrestrial stock is calculated as the quadratic sum of errors on the active and inert pools. For the LGM, the errors on the global terrestrial and oceanic stocks are constrained simultaneously by the change in ^{13}C isotopic composition of ocean carbonates. The size of the active and inert terrestrial stocks during the LGM is separated through an optimization model of regional carbon stocks and areas of five 'mega-biomes' (see text and Supplementary Information).

stock. Recent work[37–39] indeed showed that high-latitude peat and other permafrost carbon stores collectively account for as much as 1,600 Pg C. Adding this stock to the 'conventional' inventories of carbon in vegetation and soils increases the total estimated PRE terrestrial carbon storage to close to 4,000 Pg C (Table 1), compared with earlier estimates of around 2,300 Pg C. On glacial–interglacial timescales, the high-latitude carbon stocks, characterized by long formation times, cannot be considered as static. The formation of high-latitude peat carbon deposits is for instance estimated to have been slowly accumulating about 400 Pg C since the deglacial warming[40]. Conversely, widespread cold steppes could have stored more carbon at the LGM, and lost it during the deglacial warming, thus contributing to the observed atmospheric CO_2 rise. Exposed continental margins could also have stored extra carbon on land at the LGM, as evidenced by relics of terrigeneous organic carbon on the Siberian sea shelves[41].

The inferred LGM ocean carbon stock of 37,350 ± 400 Pg C places constraints on reconstructions of the global ocean circulation and biological activity. For instance, among the six different plausible ocean circulations generated by ref. 17, only one is compatible with our results. This circulation is characterized by a strong reduction of ocean ventilation in both the Northern and Southern hemispheres, and increased deposition of iron-rich dust into the Southern Ocean.

Carbon-rich and low-productivity biomes

Through a comprehensive quantification of the global stable carbon isotopic mass balance and its uncertainties, we have arrived at a net loss of 330 Pg C for the LGM to PRE change in terrestrial carbon (Table 1). This estimate falls in the lower quartile of the range from 300 to 700 Pg C given in ref. 10 and implies only a modest reduction (of the order of 10%) in the total land carbon stock at the LGM, when compared with the PRE. On the other hand, oxygen isotopes indicate a 50% lower terrestrial GPP during the LGM. These two observations can be reconciled only if the ratio of GPP to carbon storage was much lower than today.

Despite drier conditions and ice sheets that partially covered the Northern Hemisphere continents, the prevailing biomes of the LGM must have had a high carbon density as well as low productivity. This is consistent with pollen evidence for extensive tundra and cold grasslands[42], biomes that have a large below-ground carbon storage, owing to low decomposition rates; and widespread reductions in the area occupied by the most productive tropical forests with low soil carbon stock densities[43–45].

We grouped the LGM vegetation into 5 'mega-biomes', each characterized by a specific GPP flux density and a carbon stock density (Supplementary Information). The area of each mega-biome was then adjusted to best match both global GPP_{TER} and M_{TER} within their uncertainties, using a Bayesian optimization method (Supplementary Information). In the Bayesian optimization of areas, a first-guess value of each area was provided by the LPX dynamic vegetation model, prescribed with appropriately lowered CO_2 concentration and simulated LGM climate from three climate models (Supplementary Information). The results are the following. First, the optimized area covered by semi-arid and arid biomes (savannah, sclerophyll, warm grasslands and desert) is unchanged from the first guess. Second, to match both a globally low GPP_{TER} and a high M_{TER}, the LGM tropical forest area is optimized to a very low value $8 \pm 6 \times 10^6$ km^2; that is, 58% lower than the first-guess value (see Supplementary Table S2). Third, the area of tundra and cold grasslands is expanded from $32 \pm 20 \times 10^6$ km^2 in the first guess up to $45 \pm 15 \times 10^6$ km^2 in the optimization, because these biomes satisfy the dual constraint of low productivity and a high carbon density, predominantly in soils. The cited uncertainty on these estimates includes uncertainties due to the range of modelled climate.

Independent support for our mega-biome area estimates during the LGM constrained from global GPP_{TER} and M_{TER} is delivered by the BIOME-6000 database[46]. The BIOME-6000 database contains reconstructions of LGM vegetation based on pollen and plant macrofossil data for 291 sites, standardized, and then grouped into the same five 'mega-biomes' as in this study. The resulting LGM reconstructed vegetation map (Supplementary Fig. S2) confirms a significant southward expansion of tundra and cold grassland in ice-free areas of the Northern Hemisphere. Xerophytic vegetation, which includes dry grasslands, xerophytic shrublands and woodlands, and savannah replaced forests over most of the mid-latitudes of both hemispheres. Boreal forests were very reduced in extent and temperate forests (including warm-temperate variants) were largely confined to eastern North and Central America, China and Southeast Asia. Tropical forests were reduced in extent by the encroachment of xerophytic vegetation and temperate forests, consistent with the inversion results.

Another key finding from the optimization of mega-biome areas is that a stock of around 2,300 ± 300 Pg C of 'inert' terrestrial carbon (Table 1) is required to match GPP_{TER} and M_{TER}. This 'inert' pool is 700 Pg C larger than today's known permafrost and peat deposits. We speculate that it consisted mainly of organic matter embedded in permanently frozen soils of northern regions during the LGM, that is, Siberia and the exposed Arctic shelf. Although northern peatlands are thought to have been restricted at the LGM, widespread cold steppes contained large permafrost C stocks. It has been inferred[14] that permafrost soils of 'Mammoth Steppes' could have stored up to 1,000 Pg C more carbon during the LGM than today. From a palaeosol sequence in Eastern Siberia, a permafrost soil C density of 30 kg C m^{-2} was measured[47]. Scaled up to an extra 10×10^6 km^2 permafrost during LGM, this would explain an extra LGM permafrost pool of 300 Pg C in Siberia alone. A third independent estimate comes from the carbon density observed in today's turbel soils in the permafrost region (65 kg m^{-2} to 3 m depth in ref. 38), which are reasonable analogues of the LGM

cold and dry steppe biome because they are the coldest mineral soils and the dominant suborder in the continuous permafrost region. An extra 10×10^6 km^2 of frozen turbel soils during LGM would translate into an extra 650 Pg C pool of 'inert' land carbon during LGM, very close to the extra 700 Pg C reported in Table 1. Therefore, storage in northern permafrost soils alone during the LGM can account for the extra pool needed to close the ^{18}O and ^{13}C isotope constraints. In addition, some carbon-rich wetlands may have existed near springs on exposed continental shelves in the tropics during the LGM, although this hypothesis remains subject to high uncertainty[15].

A lesser than previously reported glacial–interglacial net increase in terrestrial carbon stocks implies a lesser outgassing of CO_2 by the ocean necessary to reproduce the observed atmospheric CO_2 increase. Our analysis of the required changes in glacial–interglacial land, ocean and atmosphere carbon stocks thus provides more robust constraints for hypotheses that seek to examine the mechanisms behind such changes.

Methods

The LGM marine productivity GPP_{OCEAN} is obtained from different ocean carbon-cycle models[17–19,26,27] (Table 1), giving a value of 110 ± 30 Pg C yr^{-1}. From this estimate, the LGM terrestrial productivity GPP_{TER} is calculated using equation (1), where DE_{TER} and DE_{OCEAN} are isotopic parameters calculated with spatially explicit global biogeochemical models[28], and DE is the so-called Dole effect (enrichment of atmospheric oxygen over sea water) measured in ice-cores air bubbles.

$$DE = \frac{P_{TER}}{P_{TER}+P_{OCEAN}} DE_{TER} + \frac{P_{OCEAN}}{P_{TER}+P_{OCEAN}} DE_{OCEAN} - \varepsilon_{strato} \quad (1)$$

The small fractionation ε_{strato} (0.4‰) accounts for isotopic exchange between ozone and CO_2 in the stratosphere[22]. The terms P_{TER} and P_{OCEAN} are the gross atmospheric O_2 emissions that mirror the gross uptake of CO_2 by terrestrial and marine GPP.

The LGM carbon stocks over land ecosystems and oceans are calculated by solving the linear system of equations (2)–(3), which expresses the invariance of the stock of ^{13}C and ^{12}C in the sum of the ocean, land and atmospheric reservoirs, where δ denotes the isotopic composition of each pool ($\delta^{13}C$ in ‰ VPDB) and M is their mass, or stock.

$$M_{ATM} + M_{TER} + M_{OCEAN} = cst\,1 \quad (2)$$

$$\delta_{ATM} M_{ATM} + \delta_{TER} M_{TER} + \delta_{OCEAN} M_{OCEAN} = cst\,2 \quad (3)$$

The isotopic composition changes of ocean and terrestrial reservoirs are from palaeo-data of ocean and plant $\delta^{13}C$ changes (Supplementary Information). The PRE carbon stocks are estimated from modern inventories corrected to the PRE by removing the added fossil carbon (Supplementary Information). All uncertainties on these parameters (Supplementary Information) are propagated in the M_{TER} and M_{OCEAN} calculations from equations (2)–(3) by Monte Carlo simulations. In order of decreasing importance, the main sources of uncertainties in the values of M_{TER} and M_{OCEAN} are: first, the change in δ_{OCEAN} between the LGM and PRE, established from foraminifera in ocean cores, contributing a 1 σ uncertainty of 70 Pg C in the inferred apportionment of carbon between land and ocean; second, the PRE ocean carbon stock, established from modern inventories[48], contributing an uncertainty of 26 Pg C, which was neglected in earlier studies; and third, the pre-industrial δ_{OCEAN} value contributing an uncertainty of 15 Pg C.

The global estimates of GPP_{TER} and M_{TER} derived from equations (1)–(3) pose a dual constraint on the LGM areas of five mega-biomes. A most likely estimate of the area of each mega-biome, compatible with this global constraint, is deduced from a Bayesian optimization model (Supplementary Information). In this optimization, the first guess (a priori) values are areas of each biome calculated by the LPX dynamic vegetation model[49,50]. The vegetation model was forced by climate simulations of the Paleoclimate Modelling Intercomparison Project Phase 2 (PMIP-2) to calculate the distribution of vegetation, biomass and soil carbon stock densities, in equilibrium with climate. Three climate models, selected because the data were available in the project database in June 2009 (http://pmip2.lsce.ipsl.fr/) are IPSL, HADCM3 and MIROC. We classified the output of LPX into the five mega-biomes, plus an extra inert terrestrial pool, that can be viewed as carbon stored in permanently frozen soils and in peat. Each mega-biome is assigned its average GPP (g C m^{-2} yr^{-1}) and biomass and soil carbon density (g C m^{-2}) calculated by LPX under LGM climate and CO_2. A first guess (a priori) error of 70% is assumed for each mega-biome area, and the inert pool value is set to $1{,}000 \pm 1{,}000$ Pg C, so that its value can be optimized freely by the inversion to match the global terrestrial stock M_{TER}.

Received 12 May 2011; accepted 17 October 2011; published online 20 November 2011

References

1. Denman, K. L. *et al.* in *IPCC Climate Change 2007: The Physical Science Basis* (eds Solomon, S. *et al.*) 499–587 (Cambridge Univ. Press, 2007).
2. Adams, J. M., Faure, H., Faure-Denard, L., McGlade, J. M. & Woodward, F. I. Increases in terrestrial carbon storage from the Last Glacial Maximum to the present. *Nature* **348,** 711–714 (1990).
3. Prentice, K. & Fung, I. The sensitivity of terrestrial carbon storage to climate change. *Nature* **346,** 48–51 (1990).
4. Bird, M. I., Lloyd, J. & Farquhar, G. Terrestrial carbon storage at the LGM. *Nature* **371,** 566 (1994).
5. François, L., Faure, H. & Probst, J-L. The global carbon cycle and its changes over glacial–interglacial cycles. *Glob. Planet. Change* **33,** vii–viii (2002).
6. François, L. M. *et al.* Carbon stocks and isotopic budgets of the terrestrial biosphere at mid-Holocene and last glacial maximum times. *Chem. Geol.* **159,** 163–189 (1999).
7. Friedlingstein, P., Prentice, K. C., Fung, I. Y., John, J. G. & Brasseur, G. P. Carbon-biosphere-climate interactions in the last glacial maximum climate. *J. Geophys. Res.* **100,** 7203–7221 (1995).
8. Pedersen, T. F., Francois, R., Francois, L., Alverson, K. & McManusin, J. in *Paleoclimate, Global Change and the Future* (eds Alverson, K., Bradley, R. S. & Pedersen, T. F.) 63–83 (Springer, 2003).
9. Otto, D., Rasse, D., Kaplan, J., Warnant, P. & François, L. Biospheric carbon stocks reconstructed at the Last Glacial Maximum: Comparison between general circulation models using prescribed and computed sea surface temperatures. *Glob. Planet. Change* **33,** 117–138 (2002).
10. Prentice, I. C. & Harrison, S. P. Ecosystem effects of CO_2 concentration: Evidence from past climates. *Clim. Past* **5,** 297–307 (2009).
11. Harrison, S. P. & Prentice, I. C. Climate and CO_2 controls on global vegetation distribution at the last glacial maximum: Analysis based on palaeovegetation data, biome modelling and palaeoclimate simulations. *Glob. Change Biol.* **9,** 983–1004 (2003).
12. Friedlingstein, P., Delire, C., Müller, J. F. & Gérard, J. C. The climate induced variation of the continental biosphere: A model simulation of the last glacial maximum. *Geophys. Res. Lett.* **19,** 897–900 (1992).
13. Bond, W. J., Midgley, G. F. & Woodward, F. I. The importance of low atmospheric CO_2 and fire in promoting the spread of grasslands and savannas. *Glob. Change Biol.* **9,** 973–982 (2003).
14. Zimov, S., Schuur, E. A. G. & Chapin, F. S. Permafrost and the global carbon budget. *Science* **312,** 1612–1613 (2006).
15. Faure, H., Walter, R. C. & Grant, D. R. The coastal oasis: Ice age springs on emerged continental shelves. *Glob. Planet. Change* **33,** 47–56 (2002).
16. Kohfeld, K. E., Quere, C. L., Harrison, S. P. & Anderson, R. F. Role of marine biology in glacial–interglacial CO_2 cycles. *Science* **308,** 74–78 (2005).
17. Tagliabue, A. *et al.* Quantifying the roles of ocean circulation and biogeochemistry in governing ocean carbon-13 and atmospheric carbon dioxide at the last glacial maximum. *Clim. Past* **5,** 695–706 (2009).
18. Toggweiler, J. R. Variation of atmospheric CO_2 by ventilation of the ocean's deepest water. *Paleoceanography* **14,** 571–588 (1999).
19. Brovkin, V., Ganopolski, A., Archer, D. & Rahmstorf, S. Lowering of glacial atmospheric CO_2 in response to changes in oceanic circulation and marine biogeochemistry. *Paleoceanography* **22,** PA4202 (2007).
20. Dole, M. The relative atomic weight of oxygen in water and in air. *J. Am. Chem. Soc.* **57,** 2731 (1935).
21. Barkan, E. & Luz, B. High precision measurements of $^{17}O/^{16}O$ and $^{18}O/^{16}O$ of O_2 and O_2: Ar ratio in air. *Rapid Commun. Mass Spectrom.* **17,** 2809–2814 (2003).
22. Bender, M., Sowers, T. & Labeyrie, L. The Dole effect and its variations during the last 130,000 years as measured in the Vostok ice core. *Glob. Biogeochem. Cycles* **8,** 363–376 (1994).
23. Craig, H. & Gordon, A. *Stable Isotopes in Oceanic Studies and Paleotemperatures* 9–130 (Laboratory of Geology and Nuclear Science, 1965).
24. Gillon, J. & Yakir, D. Influence of carbonic anhydrase activity in terrestrial vegetation on the ^{18}O content of atmospheric CO_2. *Science* **291,** 2584–2587 (2001).
25. Ciais, P. *et al.* A three-dimensional synthesis study of $\delta^{18}O$ in atmospheric CO_2, 1. Surface fluxes. *J. Geophys. Res.* **102,** 5857–5872 (1997).
26. Six, K. D. & Maier-Reimer, E. Effects of plankton dynamics on seasonal carbon fluxes in an ocean general circulation model. *Glob. Biogeochem. Cycles* **10,** 559–583 (1996).
27. Bopp, L., Kohfeld, K. E., Le Quéré, C. & Aumont, O. Dust impact on marine biota and atmospheric CO_2 during glacial periods. *Paleoceanography* **18,** d1046 (2003).
28. Hoffmann, G. *et al.* A model of the Earth's Dole effect. *Glob. Biogeochem. Cycles* **18,** GB1008 (2004).
29. Beer, C. *et al.* Terrestrial gross carbon dioxide uptake: global distribution and covariation with climate. *Science* **329,** 834–838 (2010).

30. Sitch, S. *et al.* Evaluation of the terrestrial carbon cycle, future plant geography and climate-carbon cycle feedbacks using five Dynamic Global Vegetation Models (DGVMs). *Glob. Change Biol.* **14,** 2015–2039 (2008).
31. Blunier, T., Barnett, B., Bender, M. L. & Hendricks, M. B. Biological oxygen productivity during the last 60,000 years from triple oxygen isotope measurements. *Glob. Biogeochem. Cycles* **16,** 1029 (2002).
32. Friedlingstein, P. *Modélisation du cycle du carbone biosphérique et étude du couplage biophère-atmosphère* PhD thesis, Free Univ. Brussels (1995).
33. Ikeda, T. & Tajika, E. Carbon cycling and climate change during the last glacial cycle inferred from the isotope records using an ocean biogeochemical carbon cycle model. *Glob. Planet. Change* **35,** 131–141 (2003).
34. Lourantou, A. *et al.* A detailed carbon isotopic constraint on the causes of the deglacial CO_2 increase. *Glob. Biogeochem. Cycle* **24,** GB2015 (2010).
35. Bird, M. I., Llyod, J. & Farquhar, G. D. Terrestrial carbon-storage from the last glacial maximum to the present. *Chemosphere* **33,** 1675–1685 (1996).
36. Crowley, T. J. Ice age terrestrial carbon changes revisited. *Glob. Biogeochem. Cycles* **9,** 377–389 (1995).
37. Gruber, N. *et al.* in *The Global Carbon Cycle: Integrating Humans, Climate and the Natural World* Vol. 62 (eds Field, C. B. & Raupach, M.) (Island Press, 2004).
38. Tarnocai, C. *et al.* Soil organic carbon pools in the northern circumpolar permafrost region. *Glob. Biogeochem. Cycles* **23,** GB2023 (2009).
39. Ping, C-L. *et al.* High stocks of soil organic carbon in the North American Arctic region. *Nature Geosci.* **1,** 615–619 (2008).
40. Yu, Z., Loisel, J., Brosseau, D. P., Beilman, D. W. & Hunt, S. J. Global peatland dynamics since the Last Glacial Maximum. *Geophys. Res. Lett.* **37,** L13402 (2010).
41. Shakhova, N. *et al.* Extensive methane venting to the atmosphere from sediments of the East Siberian Arctic shelf. *Science* **327,** 1246–1250.
42. Bigelow, N. H. *et al.* Climatic change and Arctic ecosystems I. Vegetation changes north of 55° N between the last glacial maximum, mid-Holocene, and present. *J. Geophys. Res.* **108,** 8170 (2003).
43. Prentice, I. C. & Jolly, D. BIOME 6000 participants Mid-holocene and glacial-maximum vegetation geography of the northern continents and Africa. *J. Biogeogr.* **27,** 507–519 (2000).
44. Marchant, R. A. Pollen-based biome reconstructions for Latin America at 0, 6000 and 18 000 radiocarbon years. *Clim. Past* **5,** 725–767 (2009).
45. Pickett, E. J. Pollen-based reconstructions of biome distributions for Australia, Southeast Asia and the Pacific (SEAPAC region) at 0, 6000 and 18,000 ^{14}C yr B.P. *J. Biogeogr.* **31,** 1381–1444 (2004).
46. Prentice, I. C., Harrison, S. P. & Bartlein, P. J. Tropical forests, ice ages and the carbon cycle. *New Phytol.* **189,** 988–998 (2011).
47. Zech, R., Huang, Y., Zech, M., Tarozo, R. & Zech, W. High carbon sequestration in Siberian permafrost loess-paleosols during glacials. *Clim. Past* **7,** 501–509 (2011).
48. Key, R. M. *et al.* A global ocean carbon climatology: Results from Global Data Analysis Project (GLODAP). *Glob. Biogeochem. Cycles* **18,** GB4031 (2004).
49. Prentice, I. C. *et al.* Modeling fire and the terrestrial carbon balance. *Glob. Biogeochem. Cycles* **25,** GB3005 (2011).
50. Thonicke, K. *et al.* The influence of vegetation, fire spread and fire behaviour on global biomass burning and trace gas emissions: Results from a process-based model. *Biogeosciences* **7,** 1991–2011 (2010).
51. Street-Perrott, F. A., Huang, Y., Perrott, R. A. & Eglinton, G. in *Stable Isotopes: Integration of Biological, Ecological and Geochemical Processes* (ed. Griffiths, H.) 381–396 (BIOS Scientific Publishers, 1998).
52. Prentice, I. C. & Sykes, M. T. in *Biotic Feedbacks in the Global Climatic System: Will the warming speed the warming?* (eds Woodwell, G. M. & Mackenzie, F. T.) 304–312 (Oxford Univ. Press, 1995).
53. François, L. M. *et al.* Modelling the glacial–interglacial changes in the continental biosphere. *Glob. Planet. Change* **16-17,** 37–52 (1998).
54. Kohler, P. & Fisher, H. Simulating changes in the terrestrial biosphere during the last glacial/interglacial transition. *Glob. Planet. Change* **43,** 33–55 (2004).

Acknowledgements

The authors wish to thank J-C. Duplessy for his comments on an early version of the manuscript, and M. H. Woillez for initial discussions about LGM carbon stocks. The PMIP2/MOTIF Data Archive is supported by CEA, CNRS, the EU project MOTIF (EVK2-CT-2002-00153) and the Programme National d'Etude de la Dynamique du Climat (PNEDC). The analyses were carried out using version 08-01-2009 of the database. More information is available at http://pmip2.lsce.ipsl.fr/ and http://motif.lsce.ipsl.fr/.

Author contributions

P.C. developed the model and carried out the analyses. A.T. calculated ocean C stocks and the ^{13}C isotopic composition for the PRE. M.C. carried out the uncertainty analysis associated with the terrestrial photosynthesis estimates. I.C.P., D.I.K., M.S. and S.P.H. provided simulated biomes parameters, and S.P.H. provided vegetation reconstructions. All co-authors substantially contributed to interpreting the results and writing the paper.

Additional information

The authors declare no competing financial interests. Supplementary information accompanies this paper on www.nature.com/naturegeoscience. Reprints and permissions information is available online at http://www.nature.com/reprints. Correspondence and requests for materials should be addressed to P.C.